Synthesis and Crystal Structure of the Iron Polyphosphide FeP$_4$

By Wolfgang Jeitschko and Dieter J. Braun

Institut für Anorganische und Analytische Chemie, Universität Giessen, D-6300 Giessen, Federal Republic of Germany

Crystals of FeP$_4$ were prepared by reaction of the elemental components at elevated temperatures in silica tubes in the presence of small amounts of iodine or from a tin flux. They show a profound tendency for twinning and their crystal structure was determined from 'single-crystal' counter data of a twinned crystal. FeP$_4$ is monoclinic, space group $P2_1/c$, $a = 4\cdot619$ (1), $b = 13\cdot670$ (2), $c = 7\cdot002$ (1) Å, $\beta = 101\cdot48$ (2)°, $Z = 6$. For 877 unique structure factors, which do not overlap in reciprocal space of the twin, a final R value of $0\cdot051$ was obtained. The Fe atoms are in octahedral P coordination. The P atoms are tetrahedrally coordinated by Fe and P atoms. All near-neighbor interactions can be interpreted as two-electron bonds and thus Fe obtains low-spin d^6 configuration (formal oxidation number $+2$) in agreement with its diamagnetism. While the metal atoms in CrP$_4$ (d^4 configuration for Cr) and MnP$_4$ (Mn in d^5 configuration) form Cr chains and Mn pairs respectively, no short Fe–Fe distances exist in FeP$_4$. Like the structures of CdP$_4$ and RuP$_4$, the FeP$_4$ structure can be visualized as a layer structure with parallel sheets of linked MP$_6$ octahedra. Correspondingly the two-dimensionally extended P polyanions in these three polyphosphides consist of differently condensed, puckered, ten-membered rings.

Introduction

Recently we reported on LaFe$_4$P$_{12}$ and isotypic compounds (Jeitschko & Braun, 1977). In the course of that investigation we also studied the phosphorus-rich part of the iron–phosphorus system. We were especially interested to see whether the preparation techniques (iodine as catalyst; tin as a flux) which we have used to grow crystals of LaFe$_4$P$_{12}$, La$_6$Ni$_6$P$_{17}$ (Braun & Jeitschko, 1978a), and EuCo$_2$P$_2$ (Marchand & Jeitschko, 1978) could also be utilized to synthesize new binary polyphosphides. With these techniques we have already obtained crystals of CrP$_4$ and MnP$_4$ which previously were prepared only under pressure (Jeitschko & Donohue, 1972, 1975), as well as the new compounds RuP$_4$ and OsP$_4$ (Braun & Jeitschko, 1978b).

Besides the structurally well characterized compound FeP$_2$ (Meisel, 1934; Dahl, 1969) a 'higher' phosphide with the tentative and approximate composition FeP$_{>2\cdot6}$ was obtained by Heimbrecht & Biltz (1939). This compound, which was characterized only by a graphical representation of its X-ray powder pattern, seems to correspond to FeP$_4$ which we describe in the present paper.

Synthesis, crystal growth, and properties

In preparing phosphorus-rich compounds of the transition metals, the direct synthesis from the elemental components is difficult because of the inertness of red P at moderate (<800 K) temperatures (Schäfer &

Trenkel, 1972). At higher temperatures, however, the decomposition pressure of the polyphosphide may be exceeded. To promote reaction at moderate temperatures small amounts of iodine are frequently used as a catalyst. They may also permit chemical transport (Schäfer, 1972).

The technique of growing crystals of transition-metal–metalloid compounds from metal fluxes is old (Lebeau, 1899; Jangg & Kieffer, 1973), but in the past has found little use in preparing new polyphosphides. Jolibois (1910) has grown NiP$_2$ and NiP$_3$ crystals from a tin flux.

Confirming previous experiences, the direct synthesis of an iron phosphide with a P content exceeding the composition FeP$_2$, was not successful. By annealing powders of the elemental components in evacuated silica tubes at temperatures between 900 and 1200 K for several days, we obtained only FeP$_2$. However, by adding some iodine or about 80 at.% of tin, the new iron polyphosphide was readily prepared and identified through its X-ray powder pattern.

Starting materials were all of stated purity equal to or better than 99·9%. For the preparation with the tin flux, the components were mixed in the atomic ratios between Fe:P:Sn = 1:5:40 and 1:10:40. Typical annealing conditions varied between 1 d at 900 or 1000 K followed by slow cooling (2 to 5° h^{-1}), and 21 d at 900 K followed by quenching. The tin matrix was dissolved in moderately dilute (1:1) hydrochloric acid, which also dissolves the tin phosphides formed by the excess P. This procedure only yielded microcrystalline products.

Well-developed crystals of the new iron poly-phosphide were obtained using iodine as a catalyst. The starting composition was $Fe:P = 1:10$ and 0·2 mg iodine was used for a sample of about 130 mg in a tube with a volume of 2·5 cm³. The sample was kept at 900 K for three weeks followed by slow cooling at 5° h⁻¹. The silica tubes were not visibly attacked. The crystal used for the structure determination was taken from this sample.

The crystals were black and shiny, had acicular habit and were resistant to air and non-oxidizing acids. Their chemical composition FeP_4 was established through the structure determination. Magnetic measurements with the Faraday technique indicate diamagnetism for FeP_4.

Fig. 1. Two interpenetrating reciprocal lattices hkl and $h'k'l'$ of a twin of FeP_4. The section shown has constant $k' = -k$.

Twinning, cell dimensions, and space group

The crystals were mounted in Buerger precession and Weissenberg cameras with their needle axes parallel to the dial and rotation axes respectively. At first sight they seem to have diffraction symmetry mmm. But systematic non-space-group extinctions and slight inconsistencies in intensities of 'equivalent' diffraction spots, suggested twinning. All reflections were accounted for by a monoclinic cell (Fig. 1) which was refined from Guinier powder data. An unambiguous indexing of the many reflections in the powder pattern was accomplished by comparison with a calculated pattern after the structure was determined (Table 1).

The following lattice constants were obtained with α-quartz ($a = 4·9130$, $c = 5·4046$ Å) as standard: $a = 4·619$ (1), $b = 13·670$ (2), $c = 7·002$ (1) Å, $\beta = 101·48$ (2)°, $V = 433·3$ Å³. As it should be for twinned monoclinic crystals (Donnay & Donnay, 1959) with parallel b axes, the ratios $a^2:c^2:ac \cos \beta$ approach rational numbers (10·009:23:3·0197). The needle axes of the crystals correspond to the [101] axis of the monoclinic cell. Space-group extinctions (reflections $h0l$ are observed only for $l = 2n$, $0k0$ only for $k = 2n$) led to the unique space group $P2_1/c$ (C_{2h}^5). With $Z = 6$ formula units per cell the calculated density is 4·13 g cm⁻³.

Structure determination

The crystal used for the collection of the intensity data on a four-circle diffractometer had approximate dimensions 0·025 × 0·04 × 0·3 mm and was mounted with the needle axis approximately parallel to the ω circle of the diffractometer. Graphite-monochromatized Mo $K\alpha$ radiation was used with a scintillation counter and a pulse-height discriminator. θ–2θ scans were taken with a speed of 0·1° of 2θ s⁻¹, a scan width of 2·4° of 2θ s⁻¹, and background counts of 12 s at both ends of the scans. All reflections up to $2\theta = 80°$ of one quadrant in

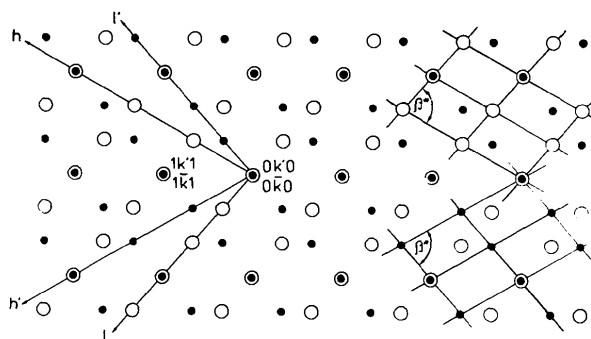## Table 1. Evaluation of a Guinier powder pattern of FeP_4 (Cu $K\alpha$ radiation)

The columns contain the Miller indices hkl, calculated and observed interplanar distances d, and relative intensities I. The calculated pattern was generated by a computer program (Yvon, Jeitschko & Parthé, 1977) using positional parameters of the refined structure.

hkl	d_c	d_o	I_c	I_o	hkl	d_c	d_o	I_c	I_o
020	6.8351	–	<1	–	-152	2.0332	–	<1	–
011	6.1329	–	1	–	230	2.0270	–	3	–
021	4.8427	4.8416	10	w	142	2.0203	–	<1	–
100	4.5265	4.5262	4	vw	211	2.0103	–	1	–
110	4.2971	4.2965	3	vw	-133	2.0015	–	<1	–
-111	3.9976	3.9974	9	w	-161	2.0005	–	2	–
031	3.7961	3.7948	8	w	-222	1.9988	1.9986	4	vw
120	3.7740	–	<1	–	221	1.9481	–	2	–
-121	3.5662	3.5651	15	m	161	1.9052	–	0	–
002	3.4311	–	<1	–	-241	1.9019 }	1.9011	3 }	w
040	3.4176	–	<1	–	043	1.9009 }		6 }	
111	3.3670	–	<1	–	-232	1.8998	–	<1	–
012	3.3279	–	1	–	062	1.8980	–	2	–
130	3.2114	–	0	–	240	1.8870	1.8868	14	m
121	3.0970	–	<1	–	071	1.8783	–	<1	–
-131	3.0804	–	1	–	113	1.8774	–	2	–
022	3.0665	–	<1	–	-143	1.8663	–	<1	–
041	3.0592	–	<1	–	231	1.8562	1.8563	4	vw
-102	3.0413	–	<1	–	152	1.8469	1.8465	7	w
-112	2.9687	2.9676	6	w	123	1.8264	–	<1	–
-122	2.7786	2.7780	33	s	-162	1.8234	–	<1	–
131	2.7627	2.7624	100	vvs	170	1.7931	–	2	–
032	2.7410	–	1	–	-242	1.7831 }	1.7825	3 }	m
140	2.7275	–	3	–	-213	1.7823 }		17 }	
-141	2.6459	–	<1	–	-171	1.7693	1.7690	8	w
051	2.5399	–	<1	–	-251	1.7551 }	1.7543	17 }	s
-132	2.5296	2.5285	32	s	053	1.7544 }		21 }	
102	2.5049	–	<1	–	133	1.7500	–	1	–
112	2.4638	–	2	–	241	1.7469	–	2	–
141	2.4363	–	<1	–	250	1.7434	1.7435	13	m
042	2.4214	2.4203	12	w	-223	1.7385	1.7386	5	w
122	2.3519	–	<1	–	202	1.7370	1.7370	30	s
150	2.3403	2.3402	4	vw	-153	1.7271	–	2	–
-151	2.2881	–	2	–	212	1.7232	–	<1	–
060	2.2784	–	<1	–	-104	1.7218	–	1	–
-142	2.2719	–	3	–	004	1.7156	–	<1	–
200	2.2633	–	<1	–	080	1.7088	–	<1	–
-211	2.2577	–	<1	–	-114	1.7083	1.7082	4	vw
013	2.2561	–	<1	–	171	1.7024	–	<1	–
210	2.2329	–	<1	–	014	1.7022	–	<1	–
-113	2.1988	2.1987	11	w	072	1.6972	1.6974	4	vw
132	2.1951	–	<1	–	162	1.6855	1.6855	14	m
-221	2.1707	–	<1	–	222	1.6835	–	0	–
023	2.1692	–	<1	–	-233	1.6722	–	<1	–
061	2.1623	–	<1	–	-124	1.6697	1.6698	13	m
220	2.1485	2.1489	3	vw	024	1.6640	1.6642	6	w
151	2.1485	–	0	–	-252	1.6605	–	<1	–
052	2.1382	2.1382	13	m	081	1.6582	1.6583	4	vw
-123	2.1182	–	<1	–	143	1.6575	1.6575	2	vw
-202	2.0901	–	<1	–	-172	1.6433	1.6433	3	vw
-212	2.0661	–	<1	–	251	1.6311	–	0	–
-231	2.0456	–	<1	–	232	1.6231	–	0	–
033	2.0443	–	<1	–	-261	1.6149 }	1.6143	10 }	m
160	2.0351	2.0353	9	w	063	1.6143 }		9 }	

reciprocal space were measured. Reflections which coincide for the two crystals of the twin (those for which $h - l = 3n$) were not used for the structure determination and refinement. Because of the small size of the crystal and the moderate linear absorption

coefficient (μ_{MoK} = 67·7 cm^{-1}) no absorption correction was made. Due to this neglect the isotropic thermal parameters B obtained in the least-squares refinement are estimated to be somewhat too low.

The structure was solved and refined with a program chain by Sheldrick (1976). Even though (due to the twinning) one third of the data were not used, it was possible to deduce some atomic positions from the Patterson map. The locations of the remaining atoms were obtained from difference Fourier syntheses. The structure was refined by a full-matrix least-squares method using scattering factors for neutral atoms (Cromer & Mann, 1968), corrected for anomalous dispersion (Cromer & Liberman, 1970). Weights were assigned according to counting statistics. No extinction correction was found necessary. The final R value for a refinement with isotropic thermal parameters is 0·051 for 877 unique structure factors with non-zero weight and counting statistics $6\sigma < F$.* A difference Fourier synthesis revealed no features lower than −1·83 e Å^{-3} or higher than 1·92 e Å^{-3}. Final parameters and interatomic distances are listed in Tables 2 and 3. The structure is shown in Figs. 2 and 3.

Discussion

The crystal structure of FeP$_4$ is of a new type and is best discussed together with the other structure types known so far for compositions MX_4 (M = metals, X = P, As). These are the structures of the transition-metal polyphosphides CrP$_4$ (with isotypic MoP$_4$), MnP$_4$ and RuP$_4$ (with isotypic OsP$_4$) already cited in the *Introduction*, the structure of CdP$_4$ (Krebs, Müller & Zürn, 1956), recently reported also for MgP$_4$ (Gibiński, Cisowska, Żdanowicz, Henkie & Wojakowski, 1974; El Maslout, Zanne, Jeannot & Gleitzer, 1975; von Schnering & Menge, 1976), and the structure of MgAs$_4$

---

* A list of observed and calculated structure factors has been deposited with the British Library Lending Division as Supplementary Publication No. SUP 33710 (11 pp.). Copies may be obtained through The Executive Secretary, International Union of Crystallography, 5 Abbey Square, Chester CH1 2HU, England.

Table 2. *Atomic parameters of* FeP$_4$

The fractional coordinates are multiplied by 10^4. Standard deviations in the least significant digits are given in parentheses.

	P2$_1$/c	x	y	z	B (Å^2)
Fe(1)	2(a)	0	0	0	0·17 (2)
Fe(2)	4(e)	1400 (3)	1699 (1)	3809 (2)	0·16 (2)
P(1)	4(e)	1975 (5)	9465 (2)	7493 (4)	0·29 (3)
P(2)	4(e)	3458 (5)	1075 (2)	1456 (3)	0·22 (2)
P(3)	4(e)	2647 (5)	8867 (2)	1962 (4)	0·33 (3)
P(4)	4(e)	3687 (5)	4447 (2)	0709 (3)	0·21 (3)
P(5)	4(e)	9256 (5)	2747 (2)	1350 (3)	0·28 (2)
P(6)	4(e)	4925 (5)	2808 (2)	4673 (3)	0·22 (2)

(Gérardin, Aubry, Courtois & Protas, 1977). In these six structural types the metal atoms are always approximately octahedrally surrounded by pnicogen (P, As) atoms, and the pnicogen atoms are all tetrahedrally coordinated; half of them by two metal and two pnicogen atoms, and the other half by one metal and three pnicogen atoms. Consequently, on average, every MX_6 octahedron needs to share four of its X atoms with other MX_6 octahedra to account for the overall composition MX_4. The differences can be seen in the various ways the MX_6 octahedra are linked *via* corners and edges, supposedly reflecting the differing bonding and space requirements of the atoms. We will discuss the bonding first.

Table 3. *Interatomic distances in* FeP$_4$ (Å)

Standard deviations are all less than 0·005 Å. Shortest distances not listed are Fe—Fe: 3·50, Fe—P: 3·49, and P—P: 2·85 Å.

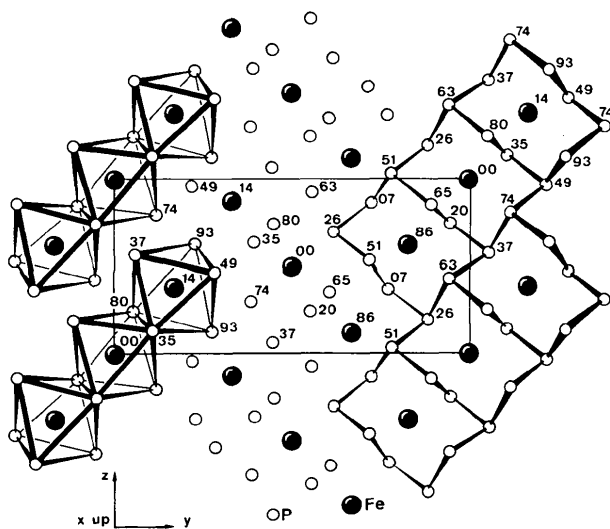| Fe(1)—2P(1)	2·255	P(3)—P(5)	2·220
2P(2)	2·259	P(4)	2·249
2P(3)	2·261	Fe(1)	2·261
		P(6)	2·275
Fe(2)—P(4)	2·187		
P(6)	2·219	P(4)—Fe(2)	2·187
P(2)	2·229	P(1)	2·189
P(1)	2·286	P(3)	2·249
P(5)	2·306	P(4)	2·285
P(5)	2·328		
		P(5)—P(3)	2·220
P(1)—P(4)	2·189	P(6)	2·241
P(2)	2·218	Fe(2)	2·306
Fe(1)	2·255	Fe(2)	2·328
Fe(2)	2·286		
		P(6)—P(2)	2·165
P(2)—P(6)	2·165	Fe(2)	2·219
P(1)	2·218	P(5)	2·241
Fe(2)	2·229	P(3)	2·275
Fe(1)	2·259		

Fig. 2. Crystal structure of FeP$_4$. In the projection along the a axis the x coordinates of the atoms are given in hundredths.
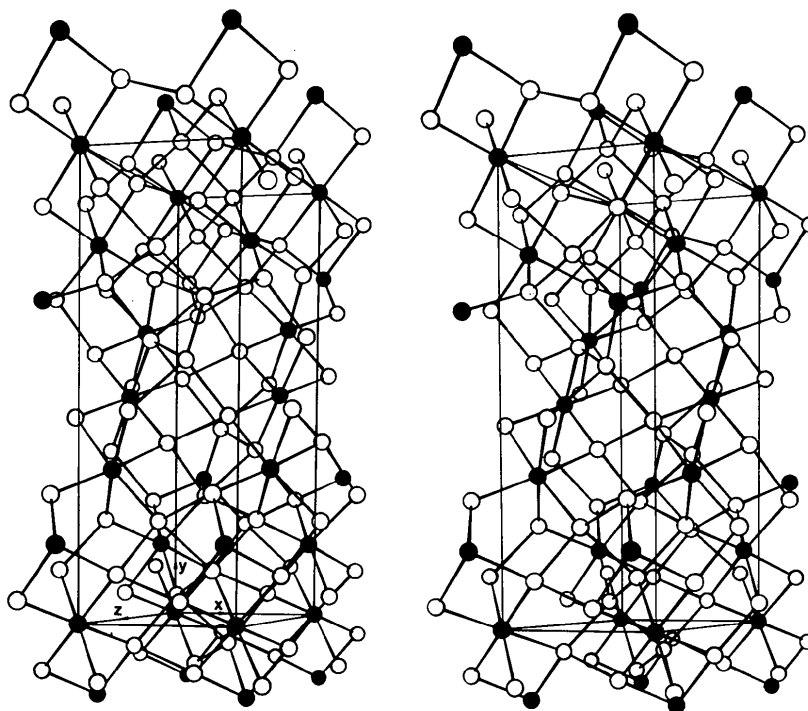
Fig. 3. Stereodiagram (Johnson, 1965) of the FeP_4 structure. Filled circles: Fe, open circles: P.

In the six structure types the metal atoms all have formal oxidation number +2. This follows simply from counting two valence electrons for all short $M-X$ and $X-X$ distances. By counting the electrons of the $M-X$ bonds as belonging to the poly-'anion' the formal charge of the metal atoms becomes +2. This counting procedure readily establishes how many valence electrons remain at the metal atoms: none at Cd and Mg, 4 at Cr, 5 at Mn, and 6 at Fe, Ru, and Os. Thus of the five d orbitals, the group VIII metals use two (e_g) orbitals for bonding (via the d^2sp^3 hybrid) and the remaining three (t_{2g}) orbitals are completely filled with the nonbonding valence electrons. This simple classical bonding model readily suggests that no metal–metal bonding is possible in the FeP_4 and RuP_4 structures: all available orbitals of the metal atoms are used for the $M-X$ bonds or completely needed to hold the remaining valence electrons. Indeed, the shortest Fe–Fe distances of 3·5 Å cannot be considered as bonding, and furthermore the distortions of the edge-shared FeP_6 octahedra are such that the Fe atoms move away from each other (Fig. 4). In that respect the RuP_4 type structure is similar to that of FeP_4. Using terms of the ligand field theory Fe is in low-spin d^6 configuration which agrees with its diamagnetism.

For CrP_4 and MnP_4 the situations are different, since the Cr and Mn atoms obtain d^4 and d^5 configurations, respectively. Thus the Cr atoms have two and the Mn atoms one state in the d orbitals available for metal–metal bonding. Through these overlapping orbitals the
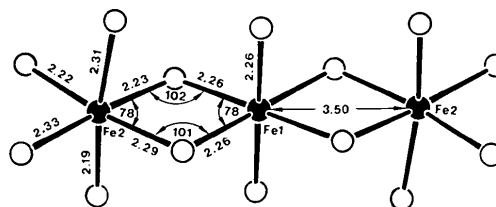

Fig. 4. Near-neighbor environments of the Fe atoms in FeP_4. Distances are given in Å, angles in degrees of arc. The Fe(1) atom is centrosymmetric.

Cr atoms form infinite Cr–Cr zig-zag chains and the Mn atoms form Mn–Mn pairs as discussed before (Jeitschko & Donohue, 1972, 1975). Optimal use of all available (metal–metal) bonding orbitals therefore favors continuous strings of edge-shared octahedra in CrP_4 and pairs of edge-shared octahedra for MnP_4, whereas from this point of view, no edge-sharing is required for the FeP_6 octahedra in FeP_4.

This suggests that there is an additional factor promoting edge-sharing of the MX_6 octahedra since, assuming at least some polarity of the $M-X$ bonds, point-charge models favor corner-sharing over edge-sharing. This additional factor, we suggest, has to do with the relative sizes of the M and X atoms. To make it simple, we take as the radii of the X atoms half of the $X-X$ bonding distances, i.e. $r_P = 1·11$ and $r_{As} = 1·22$ Å. The radii of the M atoms we obtain by subtracting r_x from the weighted averaged $M-X$ distances. Now we
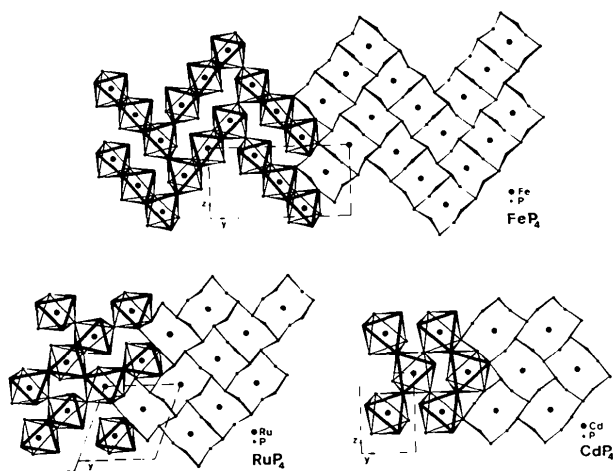
Fig. 5. Crystal structures of FeP$_4$, RuP$_4$, and CdP$_4$. Projections are along the short axes. In the left-hand parts of the drawings the linkages of the MP_6 octahedra are shown. The right-hand parts show the networks of the ten-membered rings of the phosphorus poly-'anions'.

disregard the CrP$_4$ and MnP$_4$ type structures, since they require edge-sharing to permit metal—metal bonding. Of the remaining MX_4 compounds, the highest r_M/r_X ratios (between 1·31 and 1·50) are found for CdP$_4$, MgP$_4$ and MgAs$_4$: in these compounds the MX_6 octahedra share only corners (these are also the compounds with the highest $M—X$ bond polarity, but this at least does not contradict our suggestion). FeP$_4$ with the lowest r_M/r_X ratio of 1·03, has groups of three edge-shared octahedra. In RuP$_4$ and OsP$_4$ ($r_M/r_X \simeq$ 1·15) two thirds of the MP_6 octahedra share edges (Fig. 5). MnP$_4$ with the low r_M/r_X ratio of 1·05 has groups of four edge-shared octahedra, although only Mn—Mn pairs are required (and present, because of distortions within the groups) to allow metal—metal bonding.

In summary, the FeP$_4$ structure has groups of three edge-shared FeP$_6$ octahedra. No Fe—Fe bonding is suggested from the local environments of the Fe atoms, nor is it allowed in simple bonding models. Edge-sharing of MX_6 octahedra in the MX_4 structures strongly correlates with low r_M/r_X ratios, if the other parameter (of metal—metal bonding) is accounted for. An elaboration of this argument could be achieved by least-squares refinements optimizing interatomic distances and angles (Shoemaker & Shoemaker, 1967; Meier & Villiger, 1969; Baur, 1971).

Olofsson (1965) and von Schnering & Menge (1976) have noted ten-membered P rings in the CdP$_4$ type structure. Such rings are also present in the FeP$_4$ and RuP$_4$ structures (Fig. 5). By putting the emphasis on the two-dimensionally infinite P poly-'anions', the three structures may be considered as layer structures, consisting of differently condensed ten-membered rings of P atoms, separated by the metal atoms. The linkage

of the rings is paralleled by the linking of the MP_6 octahedra via corners and edges. Other variations of this building principle seem possible.

According to our understanding of chemical bonding in FeP$_4$, we expect it to be semiconducting or semimetallic. As is the case for FeP$_4$, recent measurements on RuP$_4$ and OsP$_4$ also indicate diamagnetism for these compounds (Braun & Jeitschko, 1978c).

References

Baur, W. H. (1971). Nature (London) Phys. Sci. 233, 135–137.

Braun, D. J. & Jeitschko, W. (1978a). Acta Cryst. B34, 2069–2074.

Braun, D. & Jeitschko, W. (1978b). Z. Anorg. Allg. Chem. In the press.

Braun, D. J. & Jeitschko, W. (1978c). Unpublished results.

Cromer, D. T. & Liberman, D. (1970). J. Chem. Phys. 53, 1891–1898.

Cromer, D. T. & Mann, J. B. (1968). Acta Cryst. A24, 321–324.

Dahl, E. (1969). Acta Chem. Scand. 23, 2677–2684.

Donnay, J. D. H. & Donnay, G. (1959). International Tables for X-ray Crystallography. Vol. II. Birmingham: Kynoch Press.

El Maslout, A. Zanne, M., Jeannot, F. & Gleitzer, Ch. (1975). J. Solid State Chem. 14, 85–90.

Gérardin, R., Aubry, J., Courtois, A. & Protas, J. (1977). Acta Cryst. B33, 2091–2094.

Gibiński, T., Cisowska, E., Żdanowicz, W., Henkie, Z. & Wojakowski, A. (1974). Krist. Tech. 9, 161–163.

Heimbrecht, M. & Biltz, W. (1939). Z. Anorg. Allg. Chem. 242, 233–236.

Jangg, G. & Kieffer, R. (1973). Monatsh. Chem. 104, 226–233.

Jeitschko, W. & Braun, D. J. (1977). Acta Cryst. B33, 3401–3406.

Jeitschko, W. & Donohue, P. C. (1972). Acta Cryst. B28, 1893–1898.

Jeitschko, W. & Donohue. P. C. (1975). Acta Cryst. B31, 574–580.

Johnson, C. K. (1965). ORTEP. Report ORNL-3794. Oak Ridge National Laboratory, Tennessee.

Jolibois, P. (1910). C. R. Acad. Sci. 150, 106–108.

Krebs, H., Müller, K.-H. & Zürn, G. (1956). Z. Anorg. Allg. Chem. 285, 15–28.

Lebeau, P. (1899). C. R. Acad. Sci. 128, 933–936.

Marchand, R. & Jeitschko, W. (1978). J. Solid State Chem. 24, 351–357.

Meier, W. M. & Villiger, H. (1969). Z. Kristallogr. 129, 411–423.

Meisel, K. (1934). Z. Anorg. Allg. Chem. 218, 360–364.

Olofsson, O. (1965). Acta Chem. Scand. 19, 229–241.

SCHÄFER, H. (1972). *Preparative Methods in Solid State Chemistry*, edited by P. HAGENMULLER, pp. 251–277. New York: Academic Press.

SCHÄFER, H. & TRENKEL, M. (1972). *Z. Anorg. Allg. Chem.* **391**, 11–18.

SCHNERING, H. G. VON & MENGE, G. (1976). *Z. Anorg. Allg. Chem.* **422**, 219–225.

SHELDRICK, G. (1976). *SHELX* 76. Program system for crystal structure determination.

SHOEMAKER, C. B. & SHOEMAKER, D. P. (1967). *Acta Cryst.* **23**, 231–238.

YVON, K., JEITSCHKO, W. & PARTHÉ, E. (1977). *J. Appl. Cryst.* **10**, 73–74.

The Crystal Structures of Two Modifications of HfNi₃

BY LARS BSENKO

Institute of Chemistry, University of Uppsala, Box 531, S-751 21 Uppsala, Sweden

HfNi₃ occurs in two modifications: a high-temperature α form, stable from its melting point to 1200°C, and a low-temperature β form, stable below 1200°C. The crystal structures of the two modifications have been determined from single-crystal X-ray diffraction data. α-HfNi₃ crystallizes with the BaPb₃-type structure, space group $R\bar{3}m$ (No. 166). The parameters of the triply-primitive hexagonal unit cell are $a = 5\cdot2787$ (1), $c = 19\cdot2324$ (10) Å at room temperature. The structure can be described as a stacking of nine triangularly ordered, close-packed AB_3 layers in the sequence $ABABCBCAC$. β-HfNi₃ has the γ-Ta(Pd,Rh)₃-type structure, with a stacking of ten AB_3 layers in the sequence $ABCBCACBCB$. The space group is $P6_3/mmc$ (No. 194) and the unit-cell dimensions are $a = 5\cdot2822$ (2), $c = 21\cdot3916$ (18) Å at room temperature.

Introduction

Kirkpatrick & Larsen (1961) undertook an investigation of the Zr–Ni system and stated that the Hf–Ni system was analogous. In the region 65–80 at.% Ni they found two phases, Hf₂Ni₅ and Hf₂Ni₇, but no phase with the composition HfNi₃.

In a study of the entire Hf–Ni system, Svechnikov, Shurin & Dmitriyeva (1967) established the existence of three phases between 65 and 80 at.% Ni, namely Hf₂Ni₅, HfNi₃ and Hf₂Ni₇. HfNi₃ was said to possess the TiNi₃-type structure, but no unit-cell parameters were presented.

Bsenko (1978) investigated the Hf–Ni system in the region 65–80 at.% Ni by metallographic and X-ray methods. The existence of a phase with composition HfNi₃, forming peritectically from Hf₂Ni₇ and the melt, was confirmed. This high-temperature modification of HfNi₃ was found to be ductile, in contrast to the brittle modification obtained when the alloy is annealed at 1000°C for 120 h. The purpose of this study was to determine the crystal structures of the two modifications of HfNi₃ by single-crystal X-ray diffraction.

Experimental

Two alloys with nominal compositions Hf₀.₂₅Ni₀.₇₅ and Hf₀.₂₆Ni₀.₇₄ were prepared by arc-melting turnings of

Hf (containing 3% Zr, Koch-Light) and Ni (Specpure, Johnson Matthey & Co. Ltd) on a water-cooled Cu hearth under a purified Ar atmosphere. After the first melting the alloys were in the form of buttons, which were turned upside-down and remelted. The weight loss was less than 0·5%.

The alloy Hf₀.₂₅Ni₀.₇₅ was placed in a ZrO₂ crucible inside a silica tube. After evacuation the tube was sealed off and placed in a resistance furnace for 120 h at a temperature of 1000°C. The tube was quenched in water and the specimen cut into two pieces. After one of the pieces had been polished and etched, a metallographic examination showed that the alloy was a single phase. The other sample was crushed and small fragments were examined on a Weissenberg camera. The symmetry indicated that the space group was $P6_3mc$, $P\bar{6}2c$ or $P6_3/mmc$. The alloy Hf₀.₂₆Ni₀.₇₄ was placed in a ZrO₂ crucible and heat treated for 24 h in a resistance furnace (Hereaus) at 1300°C under very pure Ar gas. At this temperature the phase diagram shows that there is an equilibrium between the melt and the high-temperature α-HfNi₃. During the heat treatment the crystals of α-HfNi₃ grow larger. After the furnace had cooled, the specimen was cut, polished and etched, its surface showing large crystals of α-HfNi₃ surrounded by a fine eutectic. In order to isolate the ductile crystals, the sample was placed in a solution of *aqua regia*. The eutectic matrix dissolved after a few minutes and α-HfNi₃ crystals were isolated. They were